Scanning Microscopy

Volume 9 | Number 4 Article 5

11-13-1995

X-Ray Standing Wave Studies of Ad-Dimers on Si(001)

Y. Qian
Northwestern University, qian@anlsrs.msd.anl.gov

P. F. Lyman
Northwestern University

M. J. Bedzyk
Northwestern University

Scanning Microscopy, Vol. 9, No. 4, 1995 (Pages 969-980) 0891-7035/95$5.00+.25
Scanning Microscopy International, Chicago (AMF O'Hare), IL 60666 USA

X-RAY STANDING WAVE STUDIES OF AD-DIMERS ON Si(001)

Y. Qian[1,2,*], P.F. Lyman[1], and M.J. Bedzyk[1,2]

[1]Department of Materials Science and Engineering and Materials Research Center, Northwestern University, Evanston, Illinois 60208

[2]Materials Science Division, Argonne National Laboratory, Argonne, Illinois 60439

(Received for publication May 7, 1995 and in revised form November 13, 1995)

Abstract

X-ray standing waves generated by dynamical Bragg diffraction were used as an element-specific structural probe for investigating Ga and Sb adsorption on Si(001). Using the (004) and (022) reflections, we precisely measured Ga and Sb ad-dimer bond lengths and ad-dimer heights above the bulk-extrapolated Si(001) surface. The room temperature [001] thermal vibration amplitudes of Ga and Sb adatoms on Si(001) were also directly determined by combining the fundamental (004) and high-order harmonic (008) X-ray standing wave measurements. These high-resolution measurements reveal important quantitative structural information regarding the dimerized surface structures, and provide a stringent test for structural models proposed by various theoretical calcualtions. In this paper, we also give an overview of the X-ray standing wave technique and its application in investigating surface structure and dynamics.

Key Words: X-ray standing wave, Si(001), Ga, Sb, surface structure, dimer orientation, thermal vibrational amplitude.

*Address for correspondence:
Yonglin Qian,
Bldg. 223, #C202,
Argonne National Laboratory,
Argonne, IL 60439
Telephone number: (708) 252-5540
FAX number: (708) 252-7777
E-mail: qian@anlsrs.msd.anl.gov

Introduction

Investigations of atomic bonding, surface reconstruction, surface dynamics, and growth kinetics of group III and V metals on Si(001) are important for understanding the initial growth stage of III-V semiconductors on Si(001) [8, 10, 23]. Such studies can also provide valuable information for other important issues, such as, surfactant-mediated epitaxy, surface passivation, and delta-doping layers [11, 13, 24, 43].

Recently, we have carried out a series of high-resolution X-ray standing wave (XSW) measurements for group III and V metals (Ga and Sb) chemisorbed on the Si(001) surfaces [27, 35, 36, 50]. These measurements, which resolve the atomic structure, bonding geometry, and thermal vibrations for these surfaces, are reviewed in this paper. We also briefly describe the phenomenology and the methodology of the XSW technique.

Adsorption of Group III and V metals on Si(001)

The Si(001) clean surface is known to form a (2x1) dimerized reconstruction that reduces the number of dangling bonds on its bulk-truncated surface [44, 52]. When group III or V elements are deposited on Si(001), they form ad-dimers on the surface [3, 9, 19, 33, 39, 51]. Depending on coverage, adsorbate species, deposition temperature, and annealing temperature, these ad-dimers will reside at different sites on the Si(001) surface, have different orientations, and may (or may not) break the Si (2x1) reconstruction. Figure 1 illustrates possible ad-dimer symmetry sites and orientations on the Si(001) surface to be considered herein. Although group III and V elements both form ad-dimers on Si(001), the resulting surface structures are different.

Sb adsorption on Si(001)

Previous experimental investigations of Sb adsorption on Si(001) have applied a variety of techniques such as low-energy electron-diffraction (LEED) [18, 32, 40, 45], reflection high-energy electron-diffraction (RHEED) [38, 39], core level spectroscopy [38, 39], scanning tunneling microscopy (STM) [32, 39, 40], surface extended

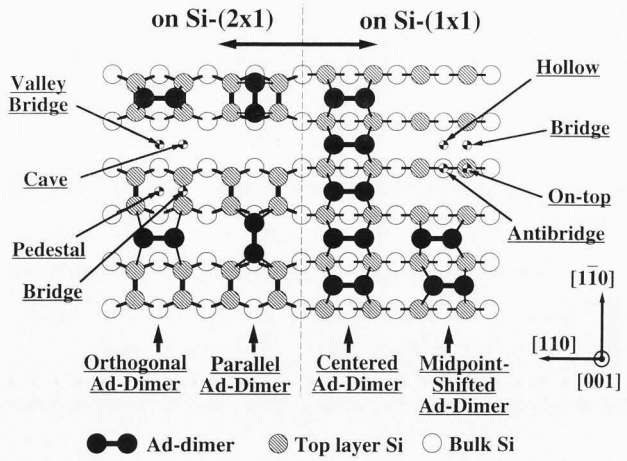

Figure 1. A schematic top view of the Si(001)-(2x1) reconstructed and (1x1) relaxed surfaces with different possible adsorption sites and orientations for group III and V ad-dimers based on symmetry.

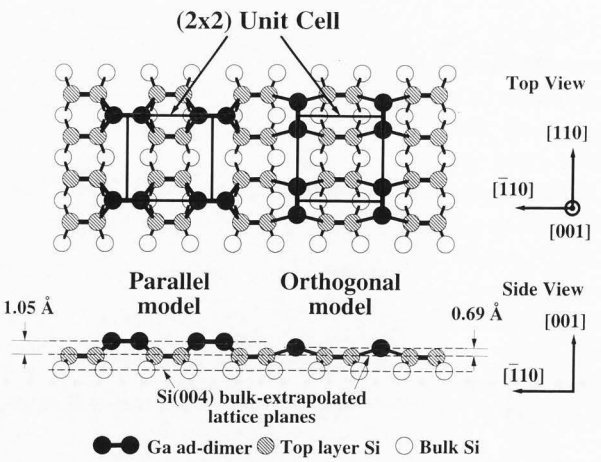

Figure 2. A top view and a side view of the parallel and orthogonal ad-dimer models for the Ga/Si(001)-(2x2) surface structure. The ad-dimer heights above the Si(001) ideal surface shown in this figure are those predicted by the DMol cluster calculations [36, 50].

X-ray absorption fine structure (SEXAFS) [40], medium energy ion scattering [45], and transmission MeV ion channeling [18]. In addition, the stability and structure have been calculated using the first principles molecular cluster approach [47] and a total energy slab calculation [53]. It is generally accepted that when Sb adsorption at 400°C saturates at nearly 1 monolayer (ML) coverage {where 1 ML = 6.78 x 10^{14} atoms/cm^2 for Si(001)}, Sb atoms form ad-dimers on top of nearly bulk-like Si with the removal of the well-known Si (2x1) dimer reconstruction, similar to the behavior of As atoms on Si(001) [51]. As illustrated in Figure 1 (right-hand side), the ad-dimers are centered at the hollow site and arranged in rows, resulting in the (1x2) symmetry. As the pentavalent Sb atoms can form three bonds (and one lone-pair orbital), and the tetravalent, top-layer Si atoms can form four bonds, there are no dangling bonds, and the surface is rather passive [11]. The saturation coverage of Sb is somewhat less than a full monolayer, ranging from 0.7 to 0.9 ML [45]. The breakup of the rows of dimers by defects and the high density of anti-phase boundaries imply a short coherence length for the domains of dimerized Sb. This explains the diffuseness and weakness of the half-order spots observed with electron diffraction. Nearest neighbor bonding distances of the Sb/Si(001)-(1x2) system have been obtained by SEXAFS [40] and measurements agree with the predicted values from theoretical calculations [47, 53]. In recent XSW measurements [27], we have precisely measured the structure and bonding geometry for the Sb/Si(001) saturated surface. In combination with the results of the above mentioned SEXAFS measurement [40], the Si surface contraction has been determined experimentally.

Ga adsorption on Si(001)

In comparison to group V, the adsorption of group III metals on Si(001)-(2x1) induces different and more complicated surface reconstructions [3, 9, 33]. Most of these reconstructions occur at coverages less than 1/2 ML. For group III adsorption on Si(001), the Ga/Si(001) surface has drawn the most attention since it is a prototype for group III metal adsorption on Si(001) and it provides valuable information about the initial stage of GaAs epitaxial growth on Si(001). Early experiments using RHEED [42], LEED and Auger electron spectroscopy (AES) [9] observed five different phases for the Ga/Si(001) surface. These five phases are: (3x2) phase at Ga coverage of 0.15-0.35 ML, (5x2) at 0.4 ML, (2x2) at 0.4-0.55 ML, (8x1) at 0.7-0.9 ML, and (1x2) at 1 ML. Based on these observations, Bourguignon *et al.* [9] proposed an orthogonal dimer model for these phases except (8x1). For the (3x2), (5x2) and (2x2) phases with the Ga coverage below 0.5 ML, the orthogonal dimer model assumes that Ga grows as ad-dimers on top of the Si (2x1) reconstructed surface and Ga ad-dimers are centered at the valley bridge site with the orientation of the Ga dimer bond perpendicular to the underlying Si dimer bond as illustrated in Figure 2. The spacing of these Ga ad-dimer rows can be arranged to form (3x2), (5x2), and (2x2) phases at coverages of 1/3, 2/5 and 1/2 ML Ga, respectively. The underlying Si reconstruction begins to be lifted when more than 0.5 ML of Ga is adsorbed on the surface, and, at Ga coverage of 1 ML, the Si(2x1) reconstruction is completely removed. In subsequent STM studies [2, 30, 31], the (3x2) and (2x2) Ga/Si(001) structures were observed for

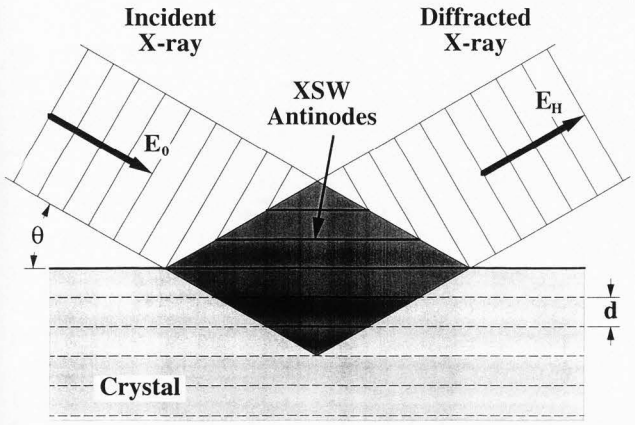

Figure 3. X-ray standing wave field generated by two-beam dynamical Bragg diffraction from a perfect single crystal.

Ga coverages below 0.5 ML. These STM images show that the Ga ad-dimers are located between the Si dimer rows and that the Ga ad-dimers grow in rows which are perpendicular to the underlying Si dimer rows. However, there were no reported STM observations of the (5x2), (8x1) and (1x2) phases.

The resolution of the above-mentioned STM measurements was not sufficient to distinguish either single Ga atoms within a Ga ad-dimer or the orientation of an ad-dimer. Therefore, besides the orthogonal ad-dimer model, the parallel ad-dimer model (Fig. 2) can also be considered consistent with the STM images and the LEED patterns. This was posed as an alternative solution for the Al/Si(001)-(2x2) surface [33]. Although the two models differ in the relative orientations of the Ga and Si dimers, both models have (2x2) symmetry at 1/2 ML and have the Ga ad-dimer located between Si dimer rows at the valley bridge site.

The orthogonal and parallel ad-dimer models were recently tested by Northrup *et al.* [34] with first-principles total-energy pseudopotential calculations for Al, Ga, and In on Si(001). For coverages below 0.5 ML, their results strongly favor the parallel model over the orthogonal model. Recent first principles molecular-cluster (DMol) calculations [36, 50] for Ga/Si(001) concur, showing that the parallel dimer model has much lower energy than the orthogonal dimer model. An impact-collision ion-scattering spectrometry experiment found that, at low coverage, In adsorbed on a vicinal Si(001) surface forms parallel ad-dimers [46]. In their STM study of the related Al/Si(001)-(2x2) system, Itoh *et al.* [22] were able to obtain atomic resolution images which confirm that Al also forms parallel ad-dimers on Si(001) at low coverage.

From DMol calculations [36, 50], the Ga ad-dimer height above the ideal Si(001) surface for the parallel model is 0.36 Å higher than the orthogonal dimer (Fig. 2). Although this slight difference may be beyond the resolution of most other techniques, the XSW method is ideally suited for this type of measurement since it is extremely sensitive to the ad-atom's height. The way we used XSW measurements to clearly rule out the orthogonal model and confirm the parallel ad-dimer model will be described later. In addition, we will also review the procedure for measuring the room temperature (RT) thermal vibrational amplitude of Ga ad-atoms on the Si(001) surface [35].

X-ray Standing Wave (XSW) Technique

Several years after its inception [4, 5], the XSW technique was developed into a powerful probe for determining the precise lattice location of ad-atoms on single crystal surfaces [7, 12, 14, 17]. It combines the advantages of X-ray diffraction, interference and fluorescence spectroscopy. Unlike conventional diffraction techniques, which lose the phase information of the structure factor, the XSW method measures both the amplitude and the phase of the Fourier components. It is also element-specific and has a high precision of typically 1% of the d-spacing of the Bragg reflection employed.

Based on the von Laue and Ewald theory for dynamical Bragg diffraction of an X-ray plane-wave from a perfect single crystal (reviewed by Batterman [6]), the interference of the coherently coupled incident and Bragg-diffracted plane waves generates an XSW in [4, 5], and above [12] the crystal, with the XSW nodal planes parallel to and having the same periodicity as the diffraction planes (see, Fig. 3). The phase of the standing wave with respect to the diffraction planes shifts by 180° as the Bragg angle θ is scanned through the arc-second wide total reflection region of the Darwin curve. This phase shift moves the antinodal planes of the standing wave inward by one-half of the d-spacing (d_{hkl}), resulting in a modulation in the photoelectron, Auger, and fluorescent yields from any atoms residing within the interference field. Thus, it can be shown that the angular dependence of the normalized fluorescence yield $Y(\theta)$ from a spatial distribution of a specific atomic species near the surface can be described as:

$$Y(\theta) = Y_{OB}\{1 + R(\theta) + 2\sqrt{R(\theta)}\, f_c \cos[v(\theta) - 2\pi P_H]\}, \quad (1)$$

where $R(\theta)$ is the reflectivity and $v(\theta)$ is the relative phase of the diffracted plane wave. The off-Bragg yield (Y_{OB}) is the fluorescence yield measured at an incident

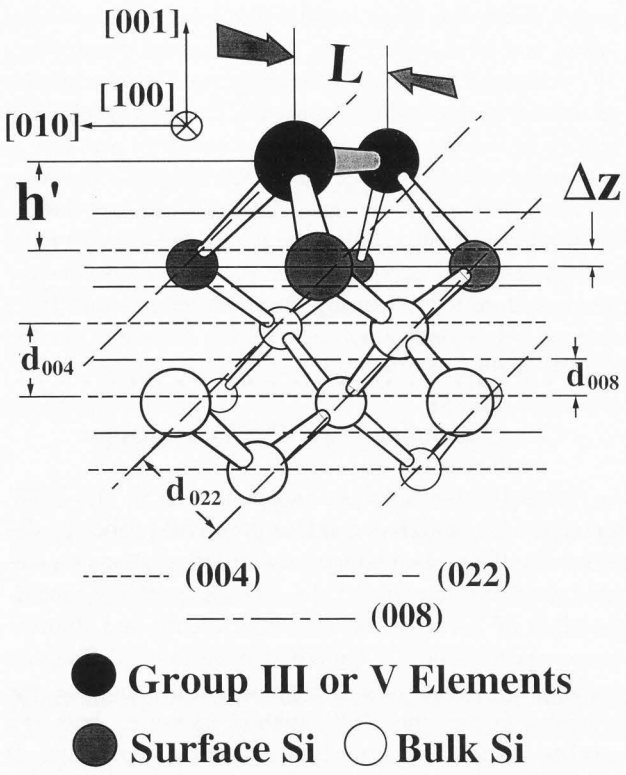

Figure 4. A side view of the group III and V adsorbed Si(001) surface ad-dimer model. The Si (004), (022) and (008) diffraction planes are represented by different dashed lines. The solid line represents the height of the relaxed Si(001) surface. h' is the ad-dimer height above the ideal Si(001) surface, Δz is the inward relaxation of the top Si layer, and L is the ad-dimer bond length. Note that the ad-dimer bond does not lie in the plane of the Figure.

---

angle ~ 1° away from the Bragg angle and can be used to calibrate the adsorbate coverage by comparison to the Y_{OB} from a standard implanted sample. The coherent fraction f_H and coherent position P_H correspond to the amplitude and phase, respectively, of the Hth Fourier component of the time-averaged spatial distribution of the nuclei of the atoms (projected into a unit cell) [20]. **H** is the reciprocal lattice vector for the (hkl) diffraction planes. Based on the convolution theorem, the coherent fraction can be written as the product of three factors [7]:

$$f_H = C\, a_H\, D_H, \tag{2}$$

where C is the fraction of atoms at ordered positions (the remaining atoms are assumed to be randomly distributed), a_H is a geometrical factor, which accounts for multiple ordered sites, and D_H is the Debye-Waller factor.

For the case of Group III and V adsorption on Si(001), the adatoms form symmetric (non-buckled) ad-dimers on Si(001) and have two equally occupied unit cell positions (see, Fig. 4). Although there are (1x2) and (2x1) domains on the Si(001) surface due to single atomic steps by which ad-dimers are rotated 90° to each other, ad-dimers in these two domains give identical positions when projected along the [001] or [022] directions. Therefore, we can analyze the problem in terms of a one-domain (1x2) structure. The coherent position is $P_{004} = h'/d_{004}$, where h' is the height of these adatoms above the Si(004) bulk-like lattice plane. Thermal vibrations smear the time-averaged spatial distribution of these adatoms. If individual atoms have a symmetrical time-averaged distribution about their mean position(s), the relation between the (008) and (004) coherent position is simply:

$$P_{008} = h'/d_{008} = 2P_{004}. \tag{3}$$

If the ad-dimer is unbuckled {i.e., parallel to the Si(001) surface}, the geometrical factors in the [001] direction are unity ($a_{004} = a_{008} = 1$). In the [022] direction, the two adatom positions have inequivalent projections, so that the geometrical factor $a_{022} = |\cos(\pi L/2d_{022})|$, where L is the ad-dimer bond length and d_{022} is the (022) diffraction plane d-spacing. Therefore, the ad-dimer bond length L can be determined as:

$$L = (2d_{022}/\pi)\cos^{-1}(-a_{022}). \tag{4}$$

As pointed out by Materlik *et al.* [28] and demonstrated by Bedzyk *et al.* [7], the XSW experiment can also measure thermal vibrational amplitudes of ad-atoms relative to the bulk lattice by employing higher-order harmonic measurements. The Debye-Waller factor can be expressed in terms of the ad-atom's thermal vibrational amplitude $(<u_H^2>)^{1/2}$ as:

$$D_H = \exp(-2\pi^2 <u_H^2>/d_H^2). \tag{5}$$

Based on eqs. (2) and (5), if the ordered fraction (C) remains constant during the combined (004) and (008) XSW measurements, the thermal vibrational amplitude along the [001] direction can be determined from the measured (004) and (008) coherent fractions as:

$$(<u_{001}^2>)^{1/2} = \{d_{004}/[\sqrt{6}\,\pi]\}\ \{\ln(f_{004}/f_{008})\}^{1/2}. \tag{6}$$

The (004)-(008) XSW combination also determines the ordered fraction (C) by the following equation:

$$C = f_{004}\,[f_{004}/f_{008}]^{1/3} \tag{7}$$

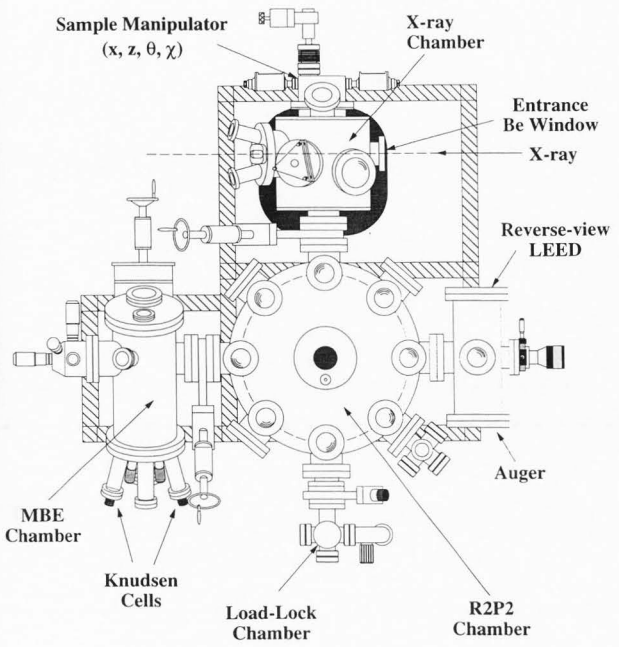

Figure 5. A top view of the UHV system at NSLS beamline X15A of Brookhaven National Laboratory.

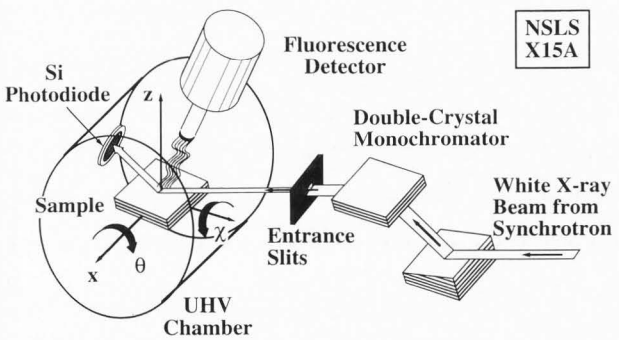

Figure 6. A schematic drawing of the XSW experimental setup at X15A.

Experimental

The experiments were conducted at beamline X15A of the National Synchrotron Light Source (NSLS) at Brookhaven National Laboratory. The X15A ultra-high vacuum (UHV) system (base pressure $\sim 9 \times 10^{-11}$ torr) consists of four coupled chambers allowing sample introduction, sample preparation {annealing, sputtering, molecular beam epitaxial (MBE) growth} and characterization (LEED, AES and XSW) (Fig. 5). The double-crystal monochromator (Fig. 6) at X15A produces a monochromated and collimated incident X-ray, which is a requirement of the XSW measurement. The X-ray beam is directed into the UHV chamber through a Be window and is Bragg reflected by the sample which is held by a UHV sample manipulator. The intensity of the Bragg-reflected X-ray beam was measured by an *in vacuo* Si photo-diode. The X-ray fluorescence yield is recorded by an energy dispersive solid-state detector (Fig. 6). In our experiments, a rocking curve about the (hkl) Bragg condition was accomplished by scanning the incident X-ray energy (using angular piezoelectric drives on both monochromator crystals). This is equivalent to scanning the angle of the sample substrate about the Bragg angle θ, and the abscissas of the data are therefore expressed as angular deflections. At each (equivalent) angular step, the reflected X-ray intensity and fluorescence spectrum were recorded simultaneously. The XSW technique as well as the experimental arrangement at X15A have recently been extensively reviewed by Zegenhagen [54].

Surface preparation

To prepare a clean Si(001)-(2x1) surface, the sample was first Syton-polished and chemically cleaned *ex situ* using the Shiraki process [21]. The sample was mounted in a strain-free manner on a molybdenum holder and was introduced into the UHV system through the load-lock chamber shown in Figure 5. After degassing the sample in UHV, the oxide layer produced by the Shiraki etch was thermally desorbed when the Si sample was flashed to 900°C for 10 minutes. The sample was then cooled to room temperature (initial cooling rate $\approx$ 2.0°C/sec), resulting in a sharp, two-domain (2x1) LEED pattern. AES could detect no O and only a small amount of C contamination ($\sim$ 0.03 ML).

To prepare the saturated Sb/Si(001) surface, $\approx$ 3 ML of Sb was deposited from an effusion cell over 10 minutes with the Si substrate held at 550° C. Since the sticking coefficient for Sb adsorption goes to zero at coverages near 1 ML [45], approximately 1 ML Sb was adsorbed on the surface. The Sb-saturated surface was further annealed for 5 minutes at 550°C, resulting in a two domain (2x1) LEED pattern with slightly diffuse half-order spots.

To prepare a Ga/Si(001) surface, Ga was evaporated from a Knudsen cell held at 830°C with the sample held at room temperature, resulting in a Ga flux of approximately 0.25 ML/min at the sample surface. We have prepared the Ga/Si(001) surfaces with various Ga coverages (Θ_{Ga}) ranging from 0.3 to 0.55 ML. For $\Theta_{Ga} <$ 1 ML, the Ga coverage was calibrated to be directly proportional to the exposure time, with a relative error of 10%. This calibration was made by using the ratio of the Ga to Si Auger peaks, and by comparison of the X-ray fluorescence yield to an ion-implanted standard sample having a known Ga areal density. We observed the LEED pattern to be (2x2) for all investigated surfaces. We did not observe the (3x2) or (5x2) LEED patterns reported by previous studies [9].

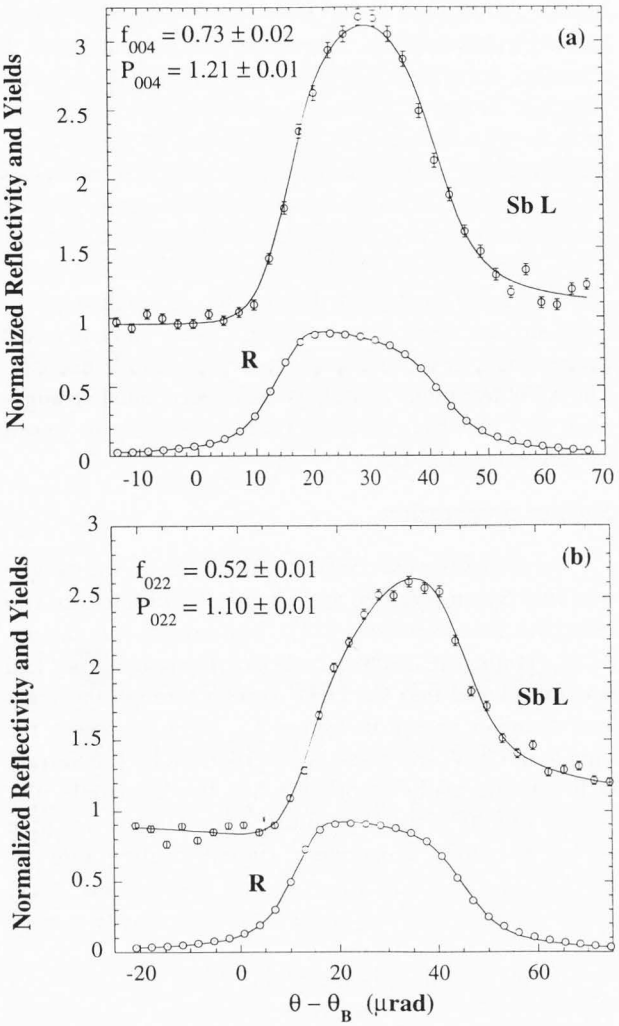

Figure 7. The experimental and theoretical angular dependence for the X-ray reflectivity and Sb L fluorescence yield for: (**a**) the (004) and (**b**) the (022) reflections.

XSW measurements

On the saturated Sb/Si(001) surface, we performed XSW measurements using the Si (004) and (022) Bragg reflections. To do the (022) measurement, the tilt angle χ of the sample had to be set at 45° from the [001] direction (which is the surface normal) towards the [010] direction (see, Fig. 4). We used 6.23 keV X-rays for the (004) measurement, and 6.77 keV X-rays for the (022) measurement (both energies are above the Sb L absorption edges). Figures 7a and 7b illustrate experimental data for the Si reflectivity and Sb L fluorescence yield as well as best fits of the dynamical diffraction theory {eq. (1)} to the experimental data for the Si (004) and (022) reflections on that surface, respectively.

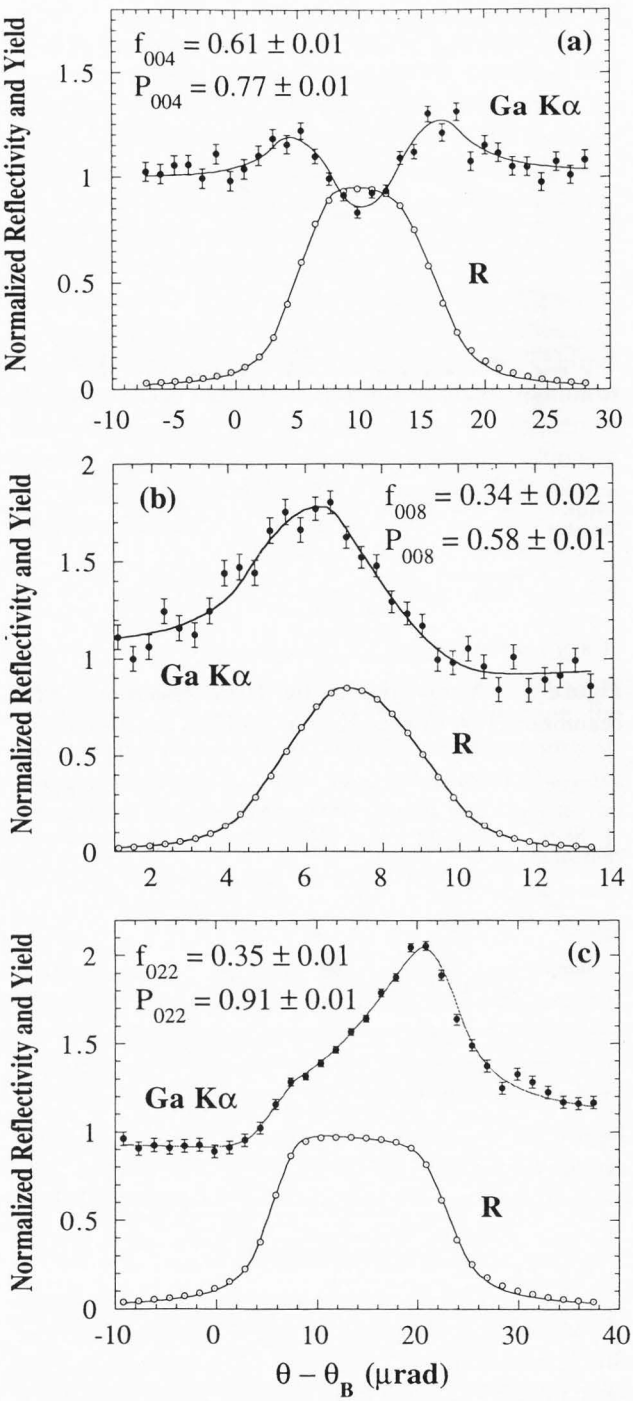

Figure 8. Experimental data (dots) and theoretical curves (solid lines) for the normalized Ga Kα fluorescence yield and Si reflectivity (R) versus Bragg reflection angle θ for: (**a**) the Si(004), (**b**) the Si(008), and (**c**) the Si(022) reflections on a 0.3 ML Ga/Si(001)-(2x2) surface.

To investigate the Ga dimer orientation and test existing theoretical models, we conducted a series of (004)

Table 1. Theoretical and experimental values of structural dimensions for the 1 ML Sb/Si(001)-(1x2) surface. L is the Sb ad-dimer bond length. h and h' are the height of the Sb ad-dimer relative to the Si(001) surface atomic plane and the Si(004) bulk-like atomic planes, respectively. Δz represents the inward relaxation of the top layer Si(001) atoms determined by comparing XSW and SEXAFS results (h' and h).

	Theory		Experiment		
	Cluster[a]	Slab (LDA)[b]	Ion Channel[c]	SEXAFS[d]	XSW[e]
L (Å)	2.93 ± 0.05	2.96	2.8 ± 0.1	2.88 ± 0.03	2.75 ± 0.06
h (Å)	1.73	1.70		1.74 ± 0.05	
h' (Å)	1.68		1.63 ± 0.07		1.64 ± 0.02
Δz = h-h' (Å)	0.05 ± 0.05		0.09 ± 0.07	0.10 ± 0.05	

[a]Ref. [47]; [b]ref. [53]; [c]ref. [18]; [d]ref. [40]; and [e]ref. [27].

XSW measurements on surfaces with various Ga coverages ranging from 0.35 ML to 0.55 ML. To measure the Ga dimer bond length and the thermal vibrational amplitude of the Ga ad-atom on Si(001) at RT, the Si (004), (022) and (008) XSW measurements were performed on the 0.3 ML Ga/Si(001) surface. For each measurement, the incident photon energy was tuned to 12.0 keV, which is above the Ga K absorption edge. During the (008) measurement, a 150-μm Al foil was placed in front of the monochromator to attenuate the coexisting 6.0 keV photons from the (004) reflection to 1%. To double check the stability of the surface, we then took another (004) XSW measurement immediately after the (008) measurement. The (004), (008) and (022) XSW results are shown in Figure 8a, 8b and 8c, respectively.

Results and Discussion

The Sb/Si(001) surface

Substrate relaxation: The coherent fractions (f_{004}, f_{022}) and coherent positions (P_{004}, P_{022}) shown in Figures 7a and 7b are determined by χ^2 fits of eq. (1) to the Sb L fluorescence data. The measured value of P_{004} = 1.21 ± 0.01 indicates that the Sb ad-dimer height h' = $P_{004}\, d_{004}$ = 1.64 ± 0.02 Å above the Si(004) bulk-like atomic planes.

In a SEXAFS experiment, Richter *et al.* [40] measured the bond lengths for this surface system, finding a Sb-Si bond length of 2.63 ± 0.04 Å and a Sb-Sb bond length of 2.88 ± 0.03 Å. Assuming a symmetric dimer geometry, the SEXAFS values imply that the Sb ad-dimer resides 1.74 ± 0.05 Å above the surface Si plane. Our XSW measurements indicate that the center of the Sb ad-dimer is located 1.64 ± 0.02 Å above the Si (004) bulk-extrapolated lattice planes. Therefore, we can conclude that at room temperature the top layer Si atoms on the saturated Sb/Si(001)-(2x1) surface are relaxed inward by 0.10 ± 0.05 Å.

The Si surface relaxation for this surface system was also measured to be 0.09 ± 0.07 Å by an ion channeling method [18] and was predicted by the first-principles cluster calculation of Tang *et al.* [47] to be 0.05 ± 0.05 Å. These results agree very well with our XSW measurement. Our result is also consistent with the pseudopotential calculation [51] of the relaxation of the As-terminated Si(001) surface (0.09 Å), which should exhibit a relaxation comparable to the present case.

Dimer geometry: To describe the geometry of symmetric Sb dimers, we need to specify the Sb-Sb bond length L in addition to the height of the dimer bond above the surface. As shown before, we can determine this quantity using eqs. (2) and (4), if we know the Debye-Waller factor (or the thermal vibrational amplitude) for the Sb adatoms. In a separate XSW study using higher-order harmonics [37], the RT thermal vibrational amplitude of Sb on Si(001) at room temperature along the [001] direction was measured to be 0.156 ± 0.01 Å. Since there is a lack of the direct measurement of the thermal vibration along the [011] direction, we will assume that the Sb thermal vibration is isotropic for the Sb/Si(001)-(2x1) surface at room temperature. This assumption is experimentally supported by findings for the similar As/Si(001) surface [15] and theoretically supported by predictions for the Si clean surface [29]. Using this $(<u_H^2>)^{1/2}$ value, the Debye-Waller factors are D_{004} = 0.77 ± 0.03 and D_{022} = 0.88 ± 0.02. Equations (2) and (4) then lead directly to a value of the Sb-Sb bond length L of 2.75 ± 0.06 Å. The XSW result is in good agreement with that determined by ion channeling (2.8 ± 0.1 Å) [18]. It also agrees with the Sb tetrahedral covalent bond length of 2.76 Å very well. However, this value is shorter than that measured by SEXAFS (2.88 ± 0.03 Å) [40]. Calculated Sb bond lengths are also somewhat larger, namely 2.93 ± 0.05 Å [47] and 2.96 Å [53].

Table 2. The XSW measured and theoretically calculated dimer bond length L and height h' as well as the covalent radius r_{cov} for group V elements.

	XSW L (Å)	$2r_{cov}$ (Å)	Theory L (Å)	XSW h' (Å)	Theory h' (Å)
As	2.58[a]	2.40	2.52[d]	1.40[a]	1.37[d]
Sb	2.75[b]	2.76	2.93[e]	1.68[b]	1.64[e]
Bi	2.96[c]	2.92	3.16[f]	1.80[c]	1.73[f]

[a]Ref. [15]; [b]ref. [27]; [c]ref. [16];
[d]ref. [48]; [e]ref. [47]; [f]ref. [49].

Table 3. (004) XSW measurements on Ga/Si(001). Θ_{Ga}: Ga coverage; h': Ga ad-dimer height relative to (400) bulk-extrapolated atom planes; C: Ga ordered fraction.

Θ_{Ga} (ML) (±0.05)	f_{004} (±0.01)	P_{004} (±0.01)	h' (Å) (±0.02)	C (±0.03)	$C \cdot \Theta_{Ga}$ (ML)
0.35	0.73	0.76	1.03	0.89	0.31
0.40	0.69	0.75	1.02	0.84	0.34
0.45	0.67	0.75	1.02	0.82	0.37
0.50	0.55	0.76	1.03	0.67	0.34
0.55	0.54	0.76	1.03	0.66	0.36

The above calculation of the Sb dimer bond length from the XSW measured values is based on the structural model which assumes that the Sb dimers are centered with respect to the underlying substrate and parallel to the surface. However, it was recently reported that on the Sb/Ge(001) surface the mid-point of the Sb dimer was shifted along the bond direction by 0.16 Å [25]. Our value of bond length L of 2.75 ± 0.06 Å has been calculated assuming no such shift. If we assume the SEXAFS value of L (2.88 Å) to be correct and allow a midpoint shift, our results would imply that the ad-dimers have a midpoint shift of 0.28 ± 0.10 Å. Additional Fourier components {e.g., (044) and (066)} are needed to uniquely determine the correct values for these parameters.

Although it is not possible for us to conclude, on the basis of the present data alone, which of the allowed points in the family of shifted solutions is correct, we favor the symmetric-dimers model (i.e., no shift), based on its simplicity and on chemical reasoning. Thus, we compare the structural parameters derived in this study under the assumption of symmetric dimers with previous theoretical and experimental studies of this surface system (Table 1).

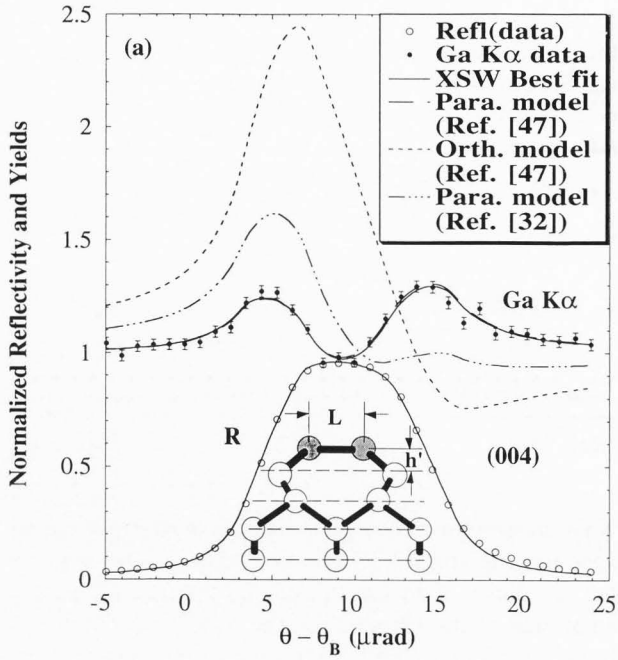

Figure 9. Experimental data and theoretical curves for the normalized Ga Kα fluorescence yield and Si reflectivity (R) versus Bragg reflection angle θ for the Si(004) reflection for the 0.55 ML Ga/Si(001) surface. Note that Tang *et al.* [50] parallel model predicted yield curve is indistinguishable from the best fit. The inset shows the [110] projected side view of the Ga/Si(001) parallel ad-dimer surface model. The model shows the Si atoms as open circles and Ga atoms as filled circles. The dashed lines represent the (004) diffraction planes in the inset.

From the result of the (004) coherent fraction of 0.73 and the (004) Debye-Waller factor of 0.77, we also conclude that the ordered fraction for the Sb/Si(001)-(2x1) surface is 95%. Highly ordered surfaces (≥ 95%) have also been observed for other group V adsorptions on Si(001) [15, 16]. These experimental results quantitatively demonstrate the nature of group V adsorption on Si(001), namely, that a highly-ordered, stable monolayer forms that passivates the Si(001) surface. This is in contrast to the behavior of group III adsorption (e.g., Ga) on Si(001) which forms a less stable and less ordered surface (see the next subsection: **The Ga/Si(001) surface**).

Besides Sb, XSW experiments have also been performed on other group V elements (namely, As and Bi) adsorbed Si(001) surfaces. To summarize structural results for the group V metals (As, Sb and Bi) adsorption on Si(001), we list values of the dimer bond lengths and the dimer heights measured by XSW experiments [15, 16, 27] and calculated by cluster calculations [47, 48,

Table 4. Theoretically calculated and measured structural parameters for the Ga ad-dimer on the Ga/Si(001)-(2x2) surface: L is the bond lengths of the Ga ad-dimer, and h' is the height of the Ga dimer above the bulk-like Si(004) surface atom plane.

	Parallel Model		Orthogonal Model		Tensor LEED	XSW
	Ref. [50]	Ref. [34]	Ref. [50]	Ref. [34]	Ref. [41]	Ref. [35]
L (Å)	2.65	2.63	2.64	2.50	2.62	2.58 ± 0.04
h' (Å)	1.05	0.92	0.69	0.60	1.02	1.05 ± 0.02

49] as well as covalent radii for As, Sb and Bi in Table 2. The measured dimer bond lengths of group V elements correspond with their covalent bond length and the heights of the dimers show an increase with respect to the size of the atom. The XSW measurements also show good agreement with theoretical predictions.

The Ga/Si(001) surface

Dimer orientation: As shown in Table 3, XSW experiments consistently measured the Ga ad-dimer height above the Si(004) bulk-like atom plane of h' = $P_{004} \cdot d_{004}$ = 1.03 ± 0.02 Å on the Ga/Si(001)-(2x2) surface with Ga coverages ranging from 0.35 to 0.55 ML. To demonstrate the sensitivity of our XSW measurement to the change in Ga height, we compare, in Figure 9, the (004) XSW experimental Ga Kα fluorescence yield from the 0.55 ML surface and our best fit to eq. (1) with the yield curves based on h' values predicted by the parallel and orthogonal model of DMol calculations [36, 50] as well as the parallel model of Northrup *et al.* [34]. For this comparison, the ordered fraction was set at the value that was determined from the best fit (C = 0.66). It can be easily seen in Figure 9 that our XSW experimental curve is in excellent agreement with that based on the parallel model of DMol calculations, and in complete disagreement with the orthogonal model which only differs in height by 0.36 Å. Furthermore, although the curve predicted by the parallel model [34] is in rough agreement, the sensitivity of the XSW measurement can easily discriminate the two theoretical predictions. Therefore, our high-resolution XSW measurements provide direct evidence for the Ga ad-atoms forming parallel dimers on the Si(001) surface at coverages below 0.5 ML. Most recently, Sakama *et al.* [41] studied the Ga/Si(001)-(2x2) surface using the tensor LEED method. Their experiments confirm our experimental results as well as theoretical predictions. The Ga dimer bond length (2.62 Å) and the dimer height above the ideal surface (1.02 Å) that they determined are in excellent agreement with our measurements. As a comparison, Table 4 provides the XSW and the tensor LEED [41] measured Ga dimer height as well as the predicted values for the orthogonal dimer model and the parallel dimer model by the pseudopotential [34] and DMol [36, 50] calculations.

Table 5. Measured and calculated thermal vibration amplitudes $(<u_H^2>)^{1/2}$ (in Å) at room temperature.

Bulk Si[a]	Si on Si(111)[b]	Si on Si(001)[c]	As on Si(001)[d]	Ga on Si(001)
0.075	0.120	0.107	0.14	0. 135

[a]Ref. [26]; [b,c]ref. [1]; [d]ref. [15].

From Table 3, it is interesting to note that as the Ga coverage was increased from 0.35 ML to 0.55 ML, the Ga ordered fraction C reduced from 0.85 to 0.63. Thus, the resulting ordered coverage $C \cdot \Theta_{Ga}$ remained constant at ≈ 0.33 ML. This feature, along with the constancy of the Ga ad-dimer bond length and height over this range of coverages, indicates that under the given growth conditions, only one ordered structure is formed and that Ga in excess of ≈ 1/3 ML is disordered and presumably forms Ga clusters. The fact that our highest ordered coverage is below the ideal value of 1/2 ML is consistent with STM images [2, 30, 31] which show vacancies, missing ad-dimer rows and antiphase domains. With the XSW technique, one can sense not only ad-atoms forming ordered structures but also disordered ad-atoms.

Thermal vibrational amplitudes: As shown in eq. (6), the Debye-Waller factor can be determined from f_{004} and f_{008} if the ordered fraction C is constant. We were able to obtain exactly the same f_{004} and P_{004} values within the range of error for both (004) scans taken before and after the (008) measurement. This indicates that the surface structure and the ordering are very stable over a long period of time (20-30 hours) required by the combined (004) and (008) measurements. With measured coherent fractions f_{004} = 0.61 ± 0.01 and f_{008} = 0.34 ± 0.02 and using eq. (6), we found that the [001] thermal vibrational amplitude of the Ga ad-atom on the Si(001) surface at room temperature is 0.135 ± 0.01 Å. From eq. (7) the corresponding Ga ordered fraction was C = 0.74 for this surface preparation.

For comparison, Table 5 lists measured and calculated values of $(<u_H^2>)^{1/2}$ for clean Si and As, Ga ad-

sorbed Si surfaces [1, 15, 26]. Our measured value of the Ga thermal vibrational amplitude is 12% larger than the calculated value of the Si(001) clean surface and 25% larger than that of the Si(111) clean surface but in a good agreement with that of the As/Si(001) surface.

As stated by eq. (3), the (008) coherent position should be ideally twice the (004) coherent position (up to modulo 1). Our measured value $P_{008} = 0.58 \pm 0.02$ is slightly (0.04) larger than that predicted from the (004) value. The (008)-determined h' value is 0.03 Å higher than the (004) value. Although this difference may not be appreciable for most structural techniques, it is near the limit of the XSW uncertainty range. From the present data, we do not have sufficient information to fully interpret this reproducible feature in our measurement. The most probable cause is an asymmetry in the bonding potential which causes the Ga ad-atom time-averaged spatial distribution to be asymmetrical in the [001] direction. In future temperature-dependent studies, we will more thoroughly explore the sensitivity of the higher-order harmonic coherent position to this anharmonicity effect.

Dimer bond length: To determine the Ga ad-dimer bond length L by eq. (4), the geometrical factor a_{022} has to be determined from the (022) measurement using eq. (2). Both experiment [15] and calculation [29] have shown that the anisotropy of the thermal vibration amplitude on Si(001) is rather small at room temperature. Lacking a (044) XSW measurement, we will assume that the Ga ad-atom has the same thermal vibration amplitude along both [001] and [022] directions. Therefore, the RT (022) Debye-Waller factor is $D_{022} = 0.91$. With the measured (022) coherent fraction of $f_{022} = 0.35 \pm 0.01$ and the ordered fraction of 0.74 determined for the 0.3 ML surface, the Ga ad-dimer bond length L is determined to be $2{,}58 \pm 0.04$ Å based on eqs. (2) and (4). The value of L predicted by cluster calculation {L = 2.65 ± 0.05 Å [50]} and by pseudo-potential calculation {2.63 Å [34]} are in good agreement with our measurement.

Conclusion and Outlook

X-ray standing wave high-resolution structural measurements for Ga and Sb adsorbed on Si(001) surfaces reveal important structural insights such as the ad-dimer orientation and bonding geometry as well as thermal vibrational amplitudes. With the advent of brighter synchrotron radiation sources such as the Advanced Photon Source and the European Synchrotron Radiation Facilities, more demanding experiments, such as *in situ* surface studies, studies of surface dynamics, or experiments of studies with only trace coverages, or kinetics of surface transformations will become feasible.

Acknowledgment

The authors would like to thank J.E. Northrup, S. Tang and A.J. Freeman for helpful discussions. This work was supported by the U.S. Department of Energy under contract No. W-31-109-ENG-38 to Argonne National Laboratory, contract No. DE-AC02-76CH00016 to National Synchrotron Light Source at Brookhaven National Laboratory, and by the National Science Foundation under contract No. DMR-9120521 to the MRC at Northwestern University. PFL is partially supported by National Institutes of Health under award No. IR01KD45295-01.

References

[1] Alerhand OL, Joannopoulos JD, Mele EJ (1989) Thermal amplitudes of surface atoms on Si(111) 2x1 and Si(001) 2x1. Phys. Rev. **B39**, 12622-12629.

[2] Baski AA, Nogami J, Quate CF (1990) Gallium growth and reconstruction on the Si(100) surface. J. Vac. Sci. Technol. **A 8**, 245-248.

[3] Baski AA, Nogami J, Quate CF (1991) Evolution of the Si(100)-2x2-In reconstruction. J. Vac. Sci. Technol. **A 2**, 1949- 1950.

[4] Batterman BW (1964) Effect of dynamical diffraction in X-ray fluorescence scattering. Phys. Rev. **133**, A759-A764.

[5] Batterman BW (1969) Detection of foreign atom sites by their X-ray fluorescence scattering. Phys. Rev. Lett. **22**, 703-705.

[6] Batterman BW, Cole H (1964) Dynamical Diffraction of X-rays by perfect crystals. Rev. Mod. Phys. **36**, 681-717.

[7] Bedzyk MJ, Materlik G (1985) Determination of the position and vibrational amplitude of an adsorbate by means of multiple-order X-ray standing wave measurements. Phys. Rev. **B 31**, 4110-4112.

[8] Biegelsen DK, Ponce FA, Smith AJ, Tramontana JC (1987) Initial stages of epitaxial growth of GaAs on (100) silicon. J. Appl. Phys. **61**, 1856-1859.

[9] Bourguignon B, Carleton KL, Leone SR (1988) Surface structures and growth mechanism of Ga on Si(100) determined by LEED and Auger electron spectroscopy. Surf. Sci. **204**, 455-472.

[10] Bringans RD, Olmstead MA, Uhrberg RIG, Bachrach RZ (1987) Formation of the interface between GaAs and Si: Implications for GaAs-on-Si heteroepitaxy. Appl. Phys. Lett. **51**, 523-525.

[11] Bringans RD, Biegelsen DK, Northrup JE, Swark LE (1993) Scanning tunneling microscopy studies of semiconductor surface passivation. Jpn. J. Appl. Phys. **32**, 1484-1492.

[12] Cowan PL, Golovchenko JA, Robbins MF

(1980) X-ray standing waves at crystal surfaces. Phys. Rev. Lett. **44**, 1680-1683.

[13] Eaglesham DJ, Unterwald FC, Jacobson DC (1993) Growth morphology and the equilibrium shape: The role of "surfactants" in Ge/Si island formation. Phys. Rev. Lett. **70**, 966-969.

[14] Fontes E, Patel JR, Comin F (1993) Direct measurement of the asymmetric dimer buckling of Ge on Si(001). Phys. Rev. Lett. **70**, 2790-2793.

[15] Franklin GE, Fontes E, Qian Y, Bedzyk MJ, Golovchenko JA, Patel JR (1994) Thermal vibration amplitudes and structure of As on Si(001). Phys. Rev. **B 50**, 7483-7487.

[16] Franklin GE, Tang S, Woicik JC, Bedzyk MJ, Freeman AJ, Golovchenko JA (1995) High-resolution structural study of Bi on Si(001). Phys. Rev. **B 52**, R5515-R5518.

[17] Golovchenko JA, Patel JR, Kaplan DR, Cowan PL, Bedzyk MJ (1982) Solution to the surface registration problem using X-ray standing waves. Phys. Rev. Lett. **49**, 560-563.

[18] Grant MW, Lyman PF, Hoogenraad JH, Seiberling LE (1992) Dimer formation in monolayer antimony films deposited at room temperature on Si(100)-2x1. Surf. Sci. Lett. **279**, L180-L184.

[19] Hanada T, Kawai M (1991) Study of successive phase transitions of the Si(001)-Bi surface by RHEED. Surf. Sci. **242**, 137-142.

[20] Hertel N, Materlik G, Zegenhagen J (1985) X-Ray standing wave analysis of bismuth implanted in Si(110). Z. Phys. **B 58**, 199-204.

[21] Ishizaka A, Shiraki Y (1986) Low temperature surface cleaning of silicon and its application to silicon MBE. J. Electrochem. Soc. **133**, 666-671.

[22] Itoh H, Itoh J, Schmid J, Ichinokawa T (1993) Structures of low-coverage phases of Al on the Si(100) surface observed by scanning tunneling microscopy. Phys. Rev. **B 48**, 14663-14666.

[23] Kroemer H (1987) Polar-on-nonpolar epitaxy. J. Cryst. Growth **81**, 193-204.

[24] LeGoues FK, Copel M, Tromp R (1989) Novel strain-induced defect in thin molecular-beam-epitaxy layers. Phys. Rev. Lett. **63**, 1826-1829.

[25] Lohmeier M, van der Vegt HA, van Silfhout RG, Vlieg E, Thornton JMC, Macdonald JE, Scholte PMLO (1992) Asymmetrical dimers on the Ge(001)-2x1-Sb surface observed using X-ray diffraction. Surf. Sci. **275**, 190-200.

[26] Lonsdale K (ed.) (1968) International Tables for X-Ray Crystallography III. Kynoch, Birmingham.

[27] Lyman PF, Qian Y, Bedzyk MJ (1995) Adsorbate structure and substrate relaxation for the Sb/Si(001)-(2x1) Surface, Surf. Sci. Lett. **325**, L385-L391.

[28] Materlik G, Zegenhagen J (1984) X-ray standing wave analysis with synchrotron radiation applied for surface and bulk systems. Phys. Lett. **104A**, 47-50.

[29] Mazur A, Pollmann J (1990) Anisotropy of the mean-square displacements at the Si(001)-(2x1) Surface. Surf. Sci. **225**, 72-80.

[30] Nogami J, Park S, Quate CF (1988) Behavior of Ga on Si(100) as studied by scanning tunneling microscopy. Appl. Phys. Lett. **53**, 2086-2088.

[31] Nogami J, Baski AA, Quate CF (1990) Behavior of gallium on vicinal Si(100) surfaces. J. Vac. Sci. Technol. **A 8**, 3520-3523.

[32] Nogami J, Baski AA, Quate CF (1991) Structure of the Sb-terminated Si(100) surface. Appl. Phys. Lett. **58**, 475-477.

[33] Nogami J, Baski AA, Quate CF (1991) Aluminum on the Si(100) surface: Growth of the first monolayer. Phys. Rev. **B 44**, 1415-1418.

[34] Northrup JE, Schabel MC, Karlsson CJ, Uhrberg RIG (1991) Structure of low-coverage phases of Al, Ga, and In on Si(100). Phys. Rev. **B 44**, 13799-13802.

[35] Qian Y, Bedzyk MJ (1995) Structure and ad-atom thermal vibrational amplitude for the 2x2 Ga/Si(001) surface. J. Vac. Sci. Technol. **A 13**, 1613-1616.

[36] Qian Y, Bedzyk MJ, Tang S, Freeman AJ, Franklin GE (1994) Resolve the Ga ad-dimer location and orientation on the Si(100) surface. Phys. Rev. Lett. **73**, 1521-1524.

[37] Qian Y, Lyman PF, Lee TL, Bedzyk MJ (1995) Thermal vibration amplitudes and structure of Sb on Si(001) by X-Ray Standing Waves. Accepted for publication by Physica B.

[38] Rich DH, Miller T, Franklin GE, Chiang TC (1989) Sb-induced bulk band transitions in Si(111) and Si(001) observed in synchrotron photoemission studies. Phys. Rev. **B 39**, 1438-1441.

[39] Rich DH, Leibsle FM, Samsavar A, Hirschorn ES, Miller T, Chiang TC (1989) Adsorption and interaction of Sb on Si(001) studied by scanning tunneling microscopy and core-level photoemission. Phys. Rev. **B 39**, 12758-12763.

[40] Richter M, Woicik JC, Nogami J, Pianetta P, Miyano KE, Baski AA, Kendelewicz T. Bouldin CE, Spicer WE, Quate CF, Lindau I (1990) Surface extended-X-ray-absorption fine structure and scanning tunneling microscopy of Si(001)2x1-Sb. Phys. Rev. Lett. **65**, 3417-3420.

[41] Sakama H, Murakami K, Nishikata K, Kawazu A (1994) Structure of a Si(100)2x2-Ga surface. Phys. Rev. **B 50**, 14977-14982.

[42] Sakamoto T, Kawanami H (1981) RHEED studies of Si(100) surface structures induced by Ga

evaporation. Surf. Sci. **111**, 177-188.

[43] Sakamoto K, Kyoya K, Miki K, Matsuhata H, Sakamoto T (1993) Which surfactant shall we choose for the heteroepitaxy of Ge/Si(001)? Bi as a surfactant with small self-incorporation. Jpn. J. Appl. Phys. **32**, L204-L206.

[44] Schlier RE, Farnsworth HE (1959) Structure and adsorption characteristics of clean surfaces of germanium and silicon. J. Chem. Phys. **30**, 917-926.

[45] Sliikerman WFJ, Zagwijn PM, van der Veen JF, Gravesteijn DJ, van de Walle GFA (1992) The interaction of Sb overlayers with Si(001). Surf. Sci. **262**, 25-32.

[46] Steel BE, Li L, Stevens JL, Tsong IST (1993) Structure of the Si(100)-(2x2)In surface. Phys. Rev. **B 47**, 9925-9927.

[47] Tang S, Freeman AJ (1993) Sb-induced passivation of the Si(100) surface. Phys. Rev. **B 47**, 1460-1465.

[48] Tang S, Freeman AJ (1993) Importance of adsorbate-adsorbate interactions for As and Sb chemisorption on Si(100). Phys. Rev. **B 48**, 8068-8075.

[49] Tang S, Freeman AJ (1994) Bi-induced reconstructions on Si(100). Phys. Rev. **B 50**, 1701-1704.

[50] Tang S, Freeman AJ, Qian Y, Franklin GE, Bedzyk MJ (1995) Combined theoretical and experimental investigation of the adsorption geometry of Ga on Si(100) at low coverage. Phys. Rev. **B 51**, 1593-1600.

[51] Uhrberg RIG, Bringans RD, Bachrach RZ, Northrup JE (1986) Symmetric arsenic dimers on the Si(100) surface. Phys. Rev. Lett. **56**, 520-523.

[52] Wolkow RA (1992) Direct observation of an increase in buckled dimers on Si(001) at low temperature. Phys. Rev. Lett. **68**, 2636-2639.

[53] Yu BD, Oshiyama A (1994) Reaction pathway for Sb-dimer rotation in conversion of Sb_4 precursors on Si(001). Phys. Rev. **B 50**, 8942-8945.

[54] Zegenhagen J (1993) Surface structure determination with X-Ray standing waves. Surf. Sci. Rep. **18**, 199-271.

Discussion with Reviewers

J. Zegenhagen: For determining the Sb-Sb dimer bond length the authors make two assumptions: (a) the randomly distributed fraction of the Sb atoms is the same normal and parallel to the surface, and (b) the Sb vibrational amplitude parallel to the surface is about equal to the vibrational amplitude of Si normal to the surface. How legitimate are these assumptions?

Authors: Regarding assumption (a): An incommensurate phase could cause a much lower in-plane coherent fraction (or ordered fraction) than that along the normal direction. However, both our XSW and LEED measurements, as well as results of previous LEED and STM experiments [32, 38, 39, 40] and calculations [47, 48], clearly show that Sb adatoms form a (1x2) phase of unbuckled ad-dimers on the Si(001) surface. There is no evidence for incommensurate phases on that surface. Therefore, this assumption is legitimate.

Regarding assumption (b): A previous XSW experiment by Franklin *et al.* [15] did not find any anisotropy for the As thermal vibration on the Si(001) surface. Lacking a direct measurement of the in-plane thermal vibration amplitude for the Sb/Si(001) surface, we assume that the Sb thermal vibration is isotropic since it is similar to the As/Si(001) system. The anisotropy of the Sb thermal vibration would indeed affect the final result of our Sb ad-dimer length measurement. Currently, we do not have any evidence of anisotropic thermal vibration for the Sb/Si(001) surface. To directly determine the thermal vibration amplitude along the [011] direction, and thereby measure the Sb ad-dimer bond length more precisely, high-order harmonic XSW measurements {(044) or (066)} are required.

J. Zegenhagen: For the whole analysis, the vibrations are considered in the harmonics approximation. Could anharmonicities have any influence on the results?

Authors: In the interpretation of the coherent fraction and the coherent position, the adatom thermal vibration is assumed to be harmonic, i.e., the individual adatom has a symmetrical Gaussian-like time-average distribution about its mean position. Based on this assumption, the Debye-Waller factor can be expressed as eq. (5) and the coherent positions of the fundamental and high-order harmonic reflections are related to each other by eq. (3). An anharmonicity of the thermal vibration would have some effects on both the coherent fraction and the coherent position since eqs. (3) and (5) no longer hold. For the systems that we studied {namely, Ga/Si(001) and Sb/Si(001)}, we did not observe any obvious anharmonicities for the thermal vibration within the uncertainty range of XSW measurements (i.e., $P_{008} = 2P_{004}$). As stated in the text, we would like to investigate this issue more precisely and thoroughly in future temperature-dependent studies.